NUMERICAL INVESTIGATION OF LAMINAR FORCED CONVECTION HEAT TRANSFER IN RECTANGULAR CHANNELS WITH DIFFERENT BLOCK GEOMETRIES USING NANOFLUIDS

by

Saeed FOROUTANI [a*,**] ***and Alireza RAHBARI*** [b*]

[a] Department of Mechanical Engineering, Tehran Science and Research Branch, Islamic Azad University, Damavand, Iran
[b] Department of Mechanical Engineering, Shahid Rajaee Teacher Training University, Tehran, Iran

Original scientific paper
https://doi.org/10.2298/TSCI150131092F

This research investigates the laminar steady-forced convection heat transfer of a Cu-water nanofluid in a 2-D horizontal channel with different block geometries attached to the bottom wall. The block geometries assumed in this research are triangular and curve blocks. The governing equations associated with the required boundary conditions are solved using finite volume method based on the SIMPLE technique and the effects of Reynolds number, nanofluid volume fraction, block geometry, and the numbers of blocks on the local and average Nusselt numbers are explored. The obtained results show that nanoparticles can effectively enhance the heat transfer in a channel. Furthermore, the local and average Nusselt number distribution is strongly dependent on the block geometry. As observed, the heat transfer augments with the increase in the Reynolds number and nanofluid volume fraction for both block geometries. It is also concluded that the average Nusselt number of the curve block is higher than that of the triangular block for different Reynolds numbers which declares the importance of the block geometry in the heat transfer enhancement.

Key words: *numerical investigation, laminar flow, heat transfer enhancement, block geometry nanofluid*

Introduction

Forced convection in a channel flow has been widely investigated due to its practical importance in different industries [1]. The recent development in this area has led to the concept of using suspended nanoparticles to enhance the heat transfer coefficient compared to the pure fluids. The reason is that the thermal conductivity of the conventional fluids is too low and the addition of nanoparticles to the pure fluid can improve the thermal conductivity of the mixture [2]. Several numerical and experimental researches have been conducted in the forced convection heat transfer using nanofluids. Young and Vafai [3] presented the experimental and numerical investigations of forced convective heat transfer of individual and arrays of multiple 2-D obstacles. The effects upon the Nusselt numbers and obstacle temperature differences of parametric changes in the Reynolds number, channel height, array configuration, and input heat flux were established in this research.

* Corresponding author, e-mail: ar.rahbari@gmail.com
** Young Researchers and Elite Club, North Tehran Branch, Islamic Azad University, Tehran, Iran

Maiga *et al*. [4] studied the forced convection flow of two types of nanofluids inside a uniformly heated tube for both laminar and turbulent regimes. It was inferred from this research that the ethylene glycol-γAl_2O_3 mixture showed a far better heat transfer enhancement than the water-γAl_2O_3 mixture. In another study, Maiga *et al*. [5] investigated the laminar forced convection flow of nanofluids for two particular geometrical configurations, namely a uniformly heated tube and a system of parallel, coaxial, and heated disks.

Heris *et al*. [6] performed an experimental research to analyze the laminar flow convective heat transfer through circular tube with constant wall temperature boundary condition. The nanofluids used in this research were CuO-water and Al_2O_3-water in different concentration ranges. In another research, Heris *et al*. [7] experimentally studied the laminar flow forced convection heat transfer of Al_2O_3-water nanofluid inside a circular tube with constant wall temperature. The Nusselt numbers of nanofluids were obtained for different nanoparticle concentrations as well as various Peclet and Reynolds numbers.

Ding *et al*. [8] carried out an experimental work on the forced convective heat transfer for different nanofluids. Possible mechanisms for the observed controversy were discussed from both microscopic and macroscopic viewpoints. The competing effects of particle migration on the thermal boundary layer thickness and that on the effective thermal conductivity were suggested to be responsible for the experimental observations.

According to the review done by Wang and Mujumdar [9], recent research over the past decades on fluid flow and heat transfer characteristics of nanofluids in forced and free convection flows and identifies opportunities for future research were summarized. In another review by the same author [10], two approaches have been adopted in most numerical studies to investigate the heat transfer characteristics of nanofluids. The first approach assumes that the continuum theory is still valid for fluids with suspended nanoparticles. The second approach uses a two-phase model for both the fluid and the solid phases.

The single phase and two-phase models have been widely used by several researchers. In this regard, Mirmasoumi and Behzadmehr [11] developed an improved numerical model for simulating the fully developed mixed convection of a nanofluid. Two-phase mixture model was used to investigate the effects of nanoparticles mean diameter on the flow parameters. It was shown that the non-uniformity of the particles distribution augmented when using larger nanoparticles. He *et al*. [12] performed a numerical study by using both single phase method and combined Euler and Lagrange method on the convective heat transfer of TiO_2 nanofluids flowing through a straight tube under the laminar flow conditions. The effects of nanoparticles concentrations, Reynolds number, and various nanoparticle sizes were investigated on the flow and the convective heat transfer behavior. Lotfi *et al*. [13] represented a two-phase Eulerian model to investigate the forced convective of a nanofluid. A single-phase model and two-phase mixture model formulations were also used for comparison. The comparison of calculated results with experimental data showed that the mixture model is more precise.

Moreover, in the recent reported work, researchers have applied the aforementioned knowledge in enhancement of cooling the electronic devices. Mohammed *et al*. [14] numerically studied the effect of using nanofluids on heat transfer and fluid flow characteristics in rectangular shaped microchannel heat sink (MCHS) for a wide range of Reynolds number. The results revealed that the presence of nanoparticles could enhance the cooling of MCHS under the extreme heat flux conditions with the optimum value of nanoparticles. Ho *et al.* [15] conducted an experiment for forced convective cooling performance of a Cu MCHS with Al_2O_3-water nanofluid as the coolant. Peyghambarzadeh *et al*. [16] used forced convective heat transfer in a water based nanofluid for improving the cooling performance of automobile radiator.

Results demonstrated that increasing the fluid circulating rate improved the heat transfer performance while the fluid inlet temperature to the radiator has trivial effects.

Several researchers have recently reported the effect of fin and blocks in channel for increasing or decreasing the natural or forced convection heat transfer. Accordingly, Yang and Chen [17] implemented the numerical simulations to analyze the influence of transient flow field structures, and the heat transfer characteristics of heated blocks in the channel with a transversely oscillating cylinder. Oztop *et al.* [18] numerically analyzed the forced convection heat transfer and fluid flow in an isothermally heated blocks located in a channel. The channel had three blocks attached on its bottom wall. The cooling air entered the channel with uniform velocity. It was obtained that insertion of a triangular cross-sectional bar enhanced the heat transfer for all Reynolds numbers.

Bakkas *et al*. [19] carried out a numerical study of laminar steady-natural convection induced in a 2-D horizontal channel provided with rectangular heating blocks, periodically mounted on its lower wall. The fluid flow, temperature fields and heat transfer rates were presented for different Rayleigh number, the blocks' spacing, the blocks' height and the relative width of the blocks. Heidary and Kermani [20] numerically studied the heat transfer and fluid flow analysis in a channel with blocks attached to bottom wall utilizing nanofluid. From this study, it was concluded that there existed a saturated number of blocks, beyond which, the average Nusselt number does not increase.

The main objective of this research in comparison with the previous studies in this area is to represent a 2-D numerical investigation of forced laminar convection in a rectangular channel containing triangular and curve blocks mounted on the bottom wall. Finally, the effects of the Reynolds number, nanofluid volume fraction, block geometry, and the number of blocks on the local and average Nusselt numbers are explored for both block geometries. The obtained results show that the block geometry definitely affects the heat transfer enhancement in the channels. The achieved results from the present research can be widely used by the manufacturers for different industrial applications.

Geometrical configuration

Figure 1 shows the schematic diagram of the rectangular channel and the boundary conditions for both block geometries. As observed, the computational domain considered in this research is a 2-D rectangular channel with height, H, and length, L, (the length to height ratio is $L/2H = 10$).

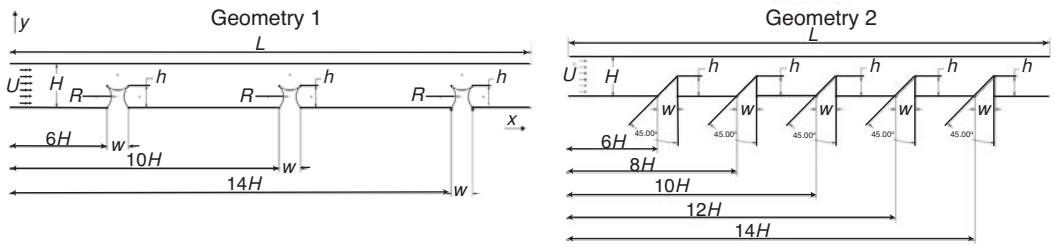

Figure 1. Schematic diagram of a physical configuration for both geometries

The Cu-water nanofluid enters the channel with uniform velocity and temperature. Moreover, the wall temperature is higher than the fluid temperature. The position of the blocks is illustrated in schematic view. Block width, w, and block height, h, are equal to $H/2$ ($w = h = H/2$).

Governing equations

The continuity, momentum, and energy equations in the Cartesian co-ordinate are written, respectively:

$$\frac{\partial u}{\partial x}+\frac{\partial v}{\partial y}=0 \tag{1}$$

$$u\frac{\partial u}{\partial x}+v\frac{\partial u}{\partial y}=-\frac{1}{\rho_{\mathrm{nf}}}\frac{\partial p}{\partial x}+\nu_{\mathrm{nf}}\left(\frac{\partial^2 u}{\partial x^2}+\frac{\partial^2 u}{\partial y^2}\right) \tag{2}$$

$$u\frac{\partial v}{\partial x}+v\frac{\partial v}{\partial y}=-\frac{1}{\rho_{\mathrm{nf}}}\frac{\partial p}{\partial x}+\nu_{\mathrm{nf}}\left(\frac{\partial^2 v}{\partial x^2}+\frac{\partial^2 v}{\partial y^2}\right) \tag{3}$$

$$u\frac{\partial T}{\partial x}+v\frac{\partial T}{\partial y}=\alpha_{\mathrm{nf}}\left(\frac{\partial^2 T}{\partial x^2}+\frac{\partial^2 T}{\partial y^2}\right) \tag{4}$$

where

$$\nu_{\mathrm{nf}}=\frac{\mu_{\mathrm{nf}}}{\rho_{\mathrm{nf}}} \tag{5}$$

$$\alpha_{\mathrm{nf}}=\frac{k_{\mathrm{nf}}}{\left(\rho c_p\right)_{\mathrm{nf}}} \tag{6}$$

Introducing the nanofluid volume fraction, φ, the dynamic viscosity, density and heat capacity of the nanofluid are calculated:

$$\mu_{\mathrm{nf}}=\frac{\mu_{\mathrm{f}}}{\left(1-\varphi\right)^{2.5}} \tag{7}$$

$$\rho_{\mathrm{nf}}=\left(1-\varphi\right)\rho_{\mathrm{f}}+\varphi\rho_{\mathrm{s}} \tag{8}$$

$$\left(\rho c_p\right)_{\mathrm{nf}}=\left(1-\varphi\right)\left(\rho c_p\right)_{\mathrm{f}}+\varphi\left(\rho c_p\right)_{\mathrm{s}} \tag{9}$$

The thermal conductivity of the fluid is estimated by Maxwell-Garnett's model:

$$\frac{k_{\mathrm{nf}}}{k_{\mathrm{f}}}=\frac{k_{\mathrm{s}}+2k_{\mathrm{f}}-2\varphi\left(k_{\mathrm{f}}-k_{\mathrm{s}}\right)}{k_{\mathrm{s}}+2k_{\mathrm{f}}+\varphi\left(k_{\mathrm{f}}-k_{\mathrm{s}}\right)} \tag{10}$$

where k_{s} and k_{f} are solid and fluid thermal conductivity, respectively.

The required boundary conditions for the equations are stated.

At the channel inlet:

$$x=0 \text{ and } 0\le y\le H \Rightarrow T=T_{\mathrm{in}}\ ,\ u=U_{\mathrm{in}}\ ,\ v=0 \tag{11}$$

At the channel outlet:

$$x=L \text{ and } 0\le y\le H \Rightarrow \frac{\partial T}{\partial x}=0\ ,\ \frac{\partial u}{\partial x}=0\ ,\ \frac{\partial v}{\partial x}=0 \tag{12}$$

At the bottom wall:

$$y = 0 \Rightarrow T = T_w, \quad u = v = 0 \tag{13}$$

At the top wall:

$$y = H \Rightarrow T = T_w, \quad u = v = 0 \tag{14}$$

On the blocks:

$$T = T_w, \quad u = v = 0 \tag{15}$$

The Reynolds number is calculated:

$$\mathrm{Re}_H = \frac{\rho_\mathrm{f} U_\mathrm{in} H}{\mu_\mathrm{f}} \tag{16}$$

The local Nusselt number along the bottom and top walls is computed from:

$$\mathrm{Nu} = -\frac{k_\mathrm{nf}}{k_\mathrm{f}} \frac{\partial T}{\partial n} \frac{H}{T_w - T_\mathrm{in}} \tag{17}$$

The average Nusselt number along the walls is calculated by integrating the local Nusselt number over the walls:

– bottom wall average Nusselt number

$$\overline{\mathrm{Nu}} = \frac{1}{s} \int_0^s \mathrm{Nu}\, \mathrm{d}s \tag{18}$$

– top wall average Nusselt number

$$\overline{\mathrm{Nu}} = \frac{1}{L} \int_0^L \mathrm{Nu}\, \mathrm{d}x \tag{19}$$

where s is the total length of the bottom wall (including the block surfaces).

Results and discussions

The numerical research has been carried out on the laminar steady-forced convection heat transfer in a 2-D horizontal channel. The Reynolds number varies from 25-150 and the nanofluid volume fraction changes from 0-20% for both block geometries.

Figure 2 shows the effects of block numbers and nanofluid volume fraction on the temperature field for both block geometries at $\mathrm{Re}_H = 100$. As observed, the thermal boundary layer thickness of the nanofluid is higher than the pure fluid ($\delta_{t,\mathrm{nf}}/\delta_{t,\mathrm{f}} > 1$) and when the nanofluid volume fraction increases, the thermal boundary layer thickness augments. This can be easily explained

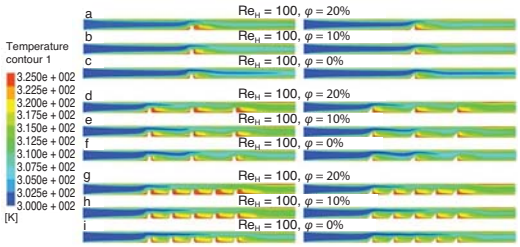

Figure 2. Temperature contour for different nanofluid volume fractions for both block geometries (*for color image see journal web site*)

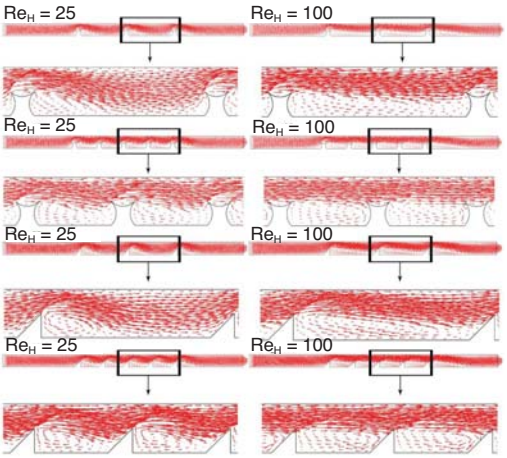

Figure 3. Velocity vectors for different Reynolds numbers for both block geometries
(*for color image see journal web site*)

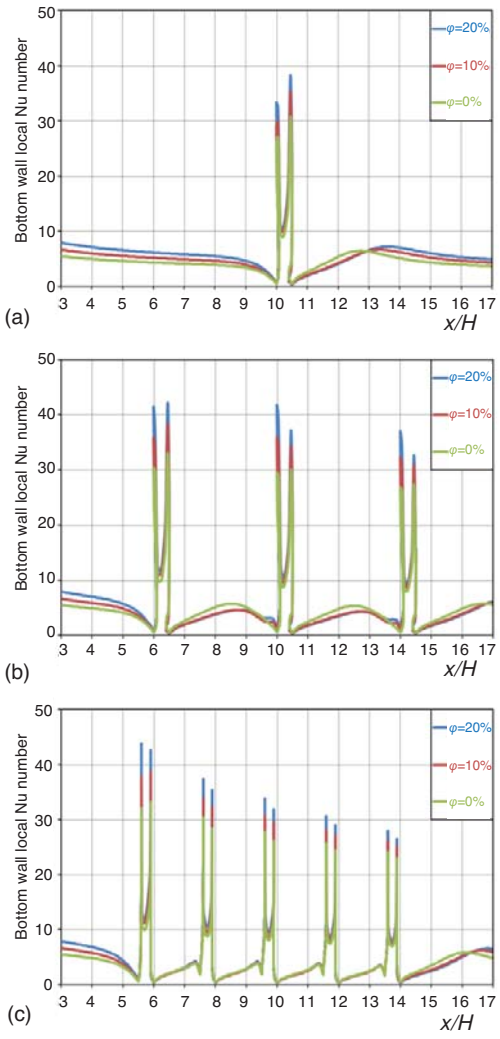

Figure 4. The effects of block numbers and φ on the Nu along the bottom wall for the first block geometry at $Re_H = 100$; (a) one block, (b) three blocks, and (c) five blocks
(*for color image see journal web site*)

by the analytical solution for a simplified case of external flow over a flat plate $\delta_t / \delta = Pr^{1/3}$ where δ is the hydrodynamics boundary layer thickness which is formulated as $\delta = 5x / (Re_x)^{1/2}$ for the laminar flow that holds this relation:

$$\frac{\delta_{t,f}}{\delta_{t,nf}} = \sqrt{\frac{\nu_f}{\nu_{nf}}} \sqrt[3]{\frac{Pr_{nf}}{Pr_f}}$$

This completely declares the reason of increasing the boundary layer thickness with φ.

Figure 3 illustrates the effect of Re_H on the velocity vector for different block numbers for both block geometries. As seen in this figure, the thermal boundary layer gravitates toward the walls as the Reynolds number increases.

Figure 4 depicts the effects of block numbers and φ on the local Nusselt number (Nu) along the bottom wall for the first block geometry at $Re_H = 100$. A dramatic surge can be perceived in the Nu when the fluid flow approaches towards the blocks because the velocity gradients and similarly the temperature gradients increase alongside the blocks. Furthermore, the Nu goes up with the rise in φ because the addition of nanoparticles to the pure fluid improves the thermal conductivity of the mixture. The comparison between the numbers of blocks in figs. 4(b) and 4(c) declares that the maximum Nu along the heated blocks occurs at the first block and then it decreases slightly along the channel. The rate of this decrease in the Nu with three blocks, fig. 4(b), is lower than the case with five blocks, fig. 4(c), because in the rectangular channel with three blocks, the fluid flow can completely recover before reaching the next block. However, in the rectangular channel with five blocks, this can not happen due to the proximity of the blocks.

Figure 5 displays the effects of block numbers and φ on the Nu along the bottom wall for the second block geometry at $Re_H = 100$. The same trend and discussion mentioned in fig. 4 is observed in fig. 5. However, compared to fig. 4, the maximum Nu takes place at the second block, fig. 5(b) and 5(c), for different nanofluid volume fractions due to the block geometry. Moreover, the range of the Nu variation is lower than that in the first block geometry.

Figures 6 and 7 reveal the effect of block numbers on the Nu along the top wall at $\varphi = 20\%$ and $Re_H = 100$ for the first and second block geometry, respectively. The maximum Nu with three and five blocks is equal for both block geometries. As expected, the Nu along the top wall is lower than that along the bottom wall.

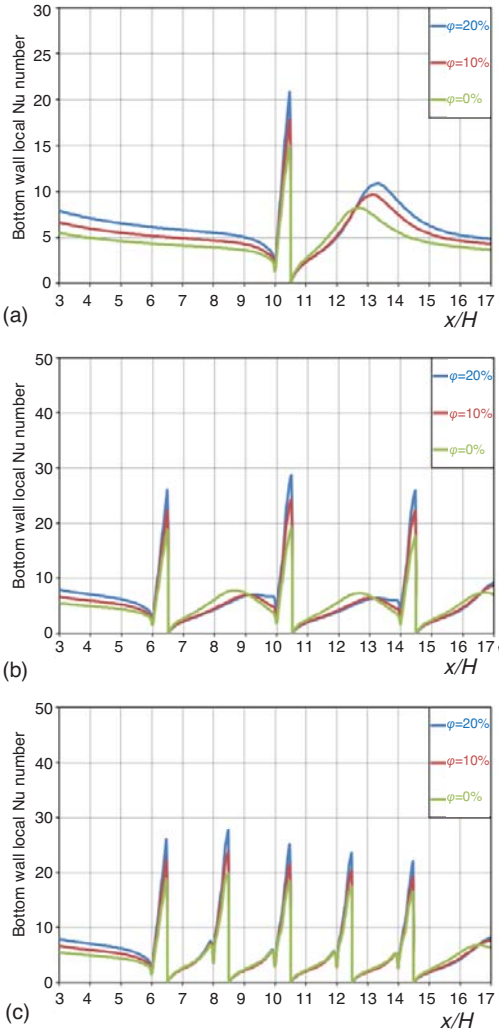

Figure 5. The effects of block numbers and φ on the Nu along the bottom wall for the second block geometry at $Re_H = 100$; (a) one block, (b) three blocks, and (c) five blocks
(*for color image see journal web site*)

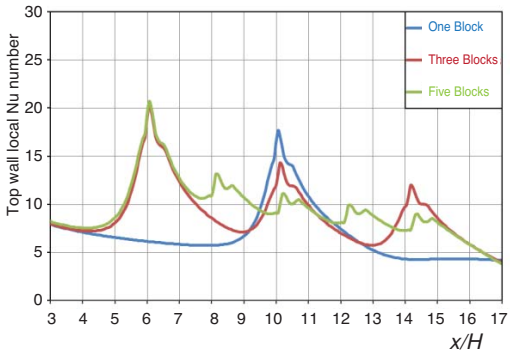

Figure 6. The effect of block numbers on the Nu along the top wall at $\varphi = 20\%$ and $Re_H = 100$ for the first block geometry
(*for color image see journal web site*)

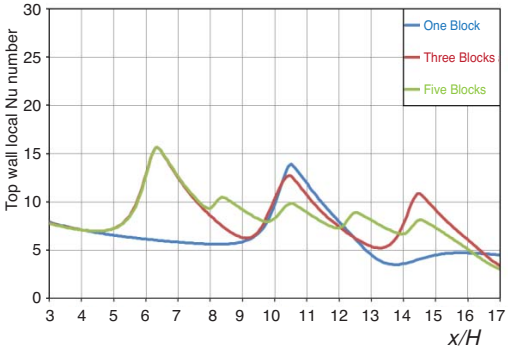

Figure 7. The effect of block numbers on the Nu along the top wall at $\varphi = 20\%$ and $Re_H = 100$ for the second block geometry
(*for color image see journal web site*)

Figure 8 shows the variation of average Nusselt number ($\overline{Nu}$) with block numbers along the bottom and top wall for the first block geometry at different φ values and $Re_H = 100$. As mentioned previously, the $\overline{Nu}$ with the increase in the block numbers and φ.

Figure 9 shows the variation of $\overline{Nu}$ with block numbers along the bottom and top wall for the second block geometry at different φ values and $Re_H = 100$. Similarly, the $\overline{Nu}$ increases with φ. Despite fig. 8 in which the $\overline{Nu}$ increases with block numbers, the bottom wall $\overline{Nu}$, fig. 9(a), goes up and down with block numbers, first increasing up to three block numbers and then decreasing in the case of five block numbers. Also, the top wall $\overline{Nu}$, fig. 9(b), increases up to three block numbers and it remains approximately constant till the five block numbers. The same trend with different block geometry was observed by [20] and it was indicated that there is a saturated number of blocks, beyond which the $\overline{Nu}$ not increase anymore and introducing more blocks with this geometry does not necessarily enhances the Nusselt number.

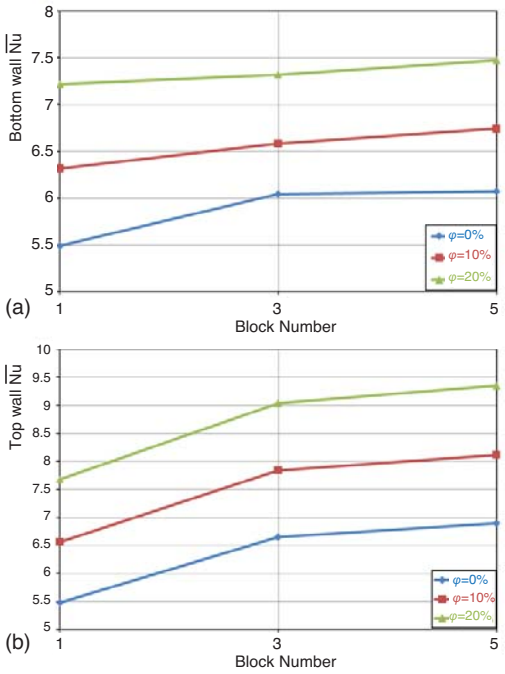

Figure 8. The variation of $\overline{Nu}$ with block numbers for the first block geometry at different φ values and $Re_H = 100$; (a) along the bottom wall, (b) along the top wall (*for color image see journal web site*)

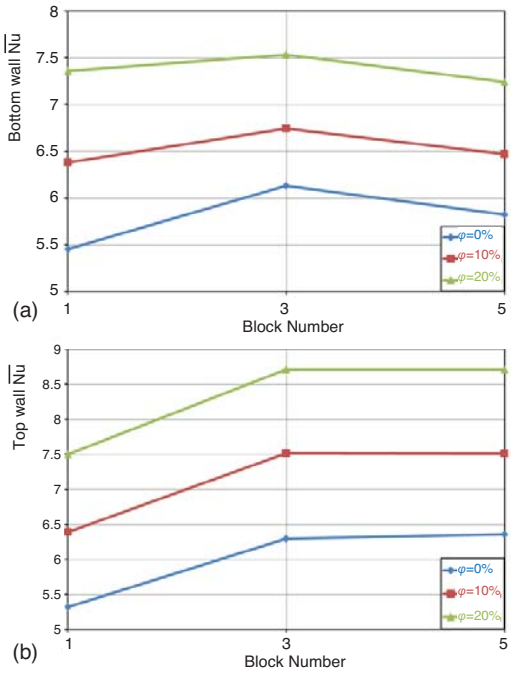

Figure 9. The variation of $\overline{Nu}$ with block numbers for the second block geometry at different φ values and $Re_H = 100$; (a) along the bottom wall, (b) along the top wall (*for color image see journal web site*)

Figure 10 depicts the variation of $\overline{Nu}$ with Re_H along the bottom and top wall for both block geometries at different φ values. As seen, the $\overline{Nu}$ increases with increase in the Re_H since the thermal boundary layer gravitates toward the walls for the higher Reynolds number. As aforementioned, the $\overline{Nu}$ augments when φ soars due to the considerable enhancement in the thermal conductivity of the mixture compared to the pure fluid. The important conclusion drawn from this figure is that the proposed first geometry demonstrates the higher $\overline{Nu}$ in contrast to the second geometry which can be widely used by the manufacturers for different industrial applications.

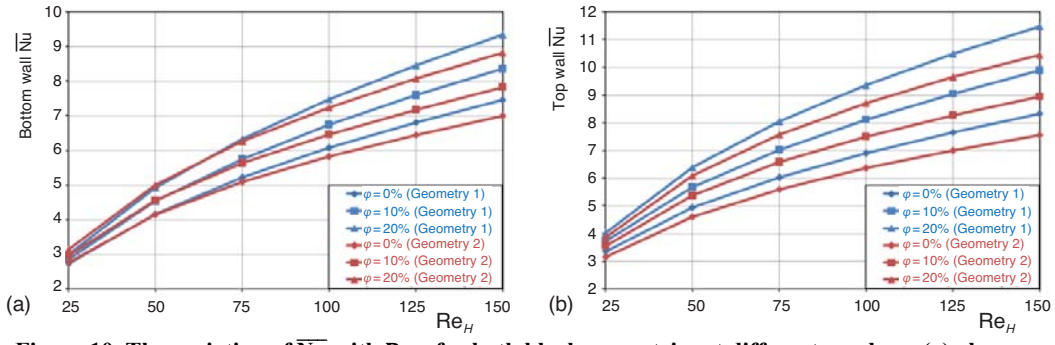

Figure 10. The variation of $\overline{Nu}$ with Re_H for both block geometries at different φ values; (a) along the bottom wall and (b) along the top wall (*for color image see journal web site*)

Conclusions

This research investigates the laminar steady-forced convection heat transfer of a Cu-water nanofluid in a rectangular channel containing curve (geometry 1) and triangular (geometry 2) blocks mounted on its bottom wall. It is observed that suspended nanoparticles can enhance the heat transfer coefficient compared to the pure fluids and when the nanofluid volume fraction, φ, varies from 0-20% for both block geometries, the local and average Nusselt number remarkably goes up. Furthermore, the average Nusselt number increases with Re_H because the thermal boundary layer gravitates toward the walls at higher Reynolds number. It is also concluded that the suggested curve block has a higher local and average Nusselt number on contrary to the triangular block. Additionally, while the maximum Nusselt number along the heated blocks occurs at the first block for the block geometry 1, it happens at the second block for the block geometry 2. Finally, the optimized block numbers for both block geometries are determined in this research. As seen, five blocks for the first block geometry and three blocks for the second block geometry are the optimum alternatives block numbers. Moreover, when the block number increases, the proximity of the blocks does not permit the fluid flow to completely recover before reaching the next block.

Nomenclature

c_p – specific heat capacity, [$\mathrm{Jkg^{-1}K^{-1}}$]
H – height of the channel, [m]
h – block height (fig. 1), [m]
h – heat transfer coefficient, [$\mathrm{Wm^{-2}K^{-1}}$]
k – thermal conductivity, [$\mathrm{Wm^{-1}K^{-1}}$]
L – length of the channel, [m]
$\underline{\mathrm{Nu}}$ – local Nusselt number, [–]
$\overline{\mathrm{Nu}}$ – average Nusselt number, [–]
p – pressure, [$\mathrm{kgm^{-1}s^{-2}}$]
Pr – Prandtl number, [–]
Re_H – Reynolds number, [–]
s – solid
T – temperature, [K]
T_{in} – inlet fluid temperature, [K]
v_{in} – inlet fluid velocity, [$\mathrm{ms^{-1}}$]
u, v – velocity component, [$\mathrm{ms^{-1}}$]

Greek symbols

α – thermal diffusivity, [$\mathrm{m^2s^{-1}}$]
μ – dynamic viscosity, [$\mathrm{kgms^{-1}}$]
ν – kinematic viscosity, [$\mathrm{m^2s^{-1}}$]
ρ – density, [$\mathrm{kgm^{-3}}$]
φ – nanofluid volume fraction, [–]

Subscripts

eff – effective
f – pure fluid
nf – nanofluid

References

[1] Demirel, Y., *et al*., Enhancement of Convection Heat Transfer in a Rectangular Duct, *Applied Energy, 64* (1999), 1-4, pp. 441-451
[2] Khanafer, K., *et al*., Buoyancy Driven Heat Transfer Enhancement in a Two-Dimensional Enclosure Utilizing Nano-Fluids, *International Journal of Heat and Mass Transfer, 46* (2003), 19, pp. 3639-3653
[3] Young, T. J., Vafai, K., Experimental and Numerical Investigation of Forced Convective Characteristics of Array of Channel Mounted Obstacles, *ASME Journal of Heat Transfer, 121* (1999), 1, pp. 34-42
[4] Maiga, S. E. B., *et al*., Heat Transfer Behaviours of Nanofluids in a Uniformly Heated Tube, *Superlattices and Microstructures, 35* (2004), 3-6, pp. 543-557
[5] Maiga, S. E. B., *et al*., Heat Transfer Enhancement by Using Nanofluids in Forced Convection Flows, *International Journal of Heat and Fluid Flow, 26* (2005), 4, pp. 530-546
[6] Heris, Z. S., *et al*., Experimental Investigation of Oxide Nanofluids Laminar Flow Convective Heat Transfer, *International Communications in Heat and Mass Transfer, 33* (2006), 4, pp. 529-535
[7] Heris, Z. S., *et al*., Experimental Investigation of Convective Heat Transfer of Al_2O_3-Water Nanofluid in Circular Tube, *International Journal of Heat and Fluid Flow, 28* (2007), 2, pp. 203-210
[8] Ding, Y., *et al.,* Forced Convective Heat Transfer of Nanofluids, *Advanced Powder Technology, 18* (2007), 6, pp. 813-824
[9] Wang, X. Q., Mujumdar, A. S., Heat Transfer Characteristics of Nanofluids: A Review, *International Journal of Thermal Science, 46* (2007), 1, pp. 1-19

[10] Wang, X. Q., Mujumdar, A. S., A Review on Nanofluids. Part 1: Theoretical and Numerical Investigations, *Brazilian Journal of Chemical Engineering, 25* (2008), 4, pp. 613–630
[11] Mirmasoumi, S., Behzadmehr, A., Effect of Nanoparticles Mean Diameter on Mixed Convection Heat Transfer of a Nanofluid in a Horizontal Tube, *International Journal of Heat and Fluid Flow, 29* (2008), 2, pp. 557-566
[12] He, Y., *et al.,* Numerical Investigation into the Convective Heat Transfer of T_iO_2 Nanofluids Flowing through a Straight Tube under the Laminar Flow Conditions, *Applied Thermal Engineering, 29* (2009), 10, pp. 1965-1972
[13] Lotfi, R., *et al*., Numerical Study of Forced Convective Heat Transfer of Nanofluids: Comparison of Different Approaches, *International Communications in Heat and Mass Transfer, 37* (2010), 1, pp. 74-78
[14] Mohammed, H., *et al*., Heat Transfer in Rectangular Microchannels Heat Sink Using Nanofluids, *International Communications in Heat and Mass Transfer, 37* (2010), 10, pp. 1496-1503
[15] Ho, C. J., *et al*., An Experimental Investigation of Forced Convective Cooling Performance of a Microchannel Heat Sink with Al_2O_3-Water Nanofluid, *Applied Thermal Engineering, 30* (2010), 2-3, pp. 96-103
[16] Peyghambarzadeh, S . M., *et al*., Improving the Cooling Performance of Automobile Radiator with Al_2O_3-Water Nanofluid, *Applied Thermal Engineering, 31* (2011), 10, pp. 1833-1838
[17] Yang, Y. T., Chen, C. H., Numerical Simulation of Turbulent Fluid Flow and Heat Transfer Characteristics of Heated Blocks in the Channel with an Oscillating Cylinder, *International Journal of Heat and Mass Transfer, 51* (2008), 7-8, pp. 1603-1612
[18] Oztop, H. F., *et al*., Control of Heat Transfer and Fluid Flow using a Triangular Bar in Heated Blocks Located in a Channel, *International Communications in Heat and Mass Transfer, 36* (2009), 8, pp. 878-885
[19] Bakkas, M., *et al*., Natural Convective Flows in a Horizontal Channel Provided with Heating Isothermal Blocks: Effect of the Inter Blocks Spacing, *Energy Conversion and Management, 51* (2010), 2, pp. 296-304
[20] Heidary, H., Kermani, M. J., Heat Transfer Enhancement in a Channel with Block(s) Effect and Utilizing Nanofluid, *International Journal of Thermal Sciences, 57* (2012), July, pp. 163-171

Paper submitted: January 31, 2015
Paper revised: June 8, 2015
Paper accepted: June 30, 2015